Uncertainty Analysis of the Hydrodynamic Coefficients Estimation of a Nonlinear Manoeuvring Model Based on Planar Motion Mechanism Tests

Haitong Xu[a], Vahid Hassani[b,c], C. Guedes Soares[a*]

[a] *Centre for Marine Technology and Ocean Engineering (CENTEC), Instituto Superior Técnico, Universidade de Lisboa, Av. Rovisco Pais, 1049-001 Lisboa, Portugal.*
[b] *Department of Marine Technology, Norwegian University of Science and Technology, 7491 Trondheim, Norway*
[c] *Department of Ships and Ocean Structures, SINTEF Ocean, Trondheim, Norway*

**Corresponding author email: c.guedes.soares@centec.tecnico.ulisboa.pt;*

ABSTRACT

Uncertainty analysis of the identified hydrodynamic coefficients of a nonlinear manoeuvring model is presented in this paper. The classical parameter estimation method, Least Square, is briefly introduced, and the uncertainty of the hydrodynamic coefficients due to the noise in the measured data is analysed using singular value decomposition. Then, two methods, truncated singular values decomposition and Tikhonov regularization, are introduced to diminish the uncertainty. A nonlinear manoeuvring mathematical model of a marine surface ship is derived using Lagrange's method. The dimensionless hydrodynamic coefficients are obtained using the Least Squares method, truncated singular values decomposition and Tikhonov regularization with Planar Motion Mechanism test data. The validation process is carried out to test the performance and accuracy of the resulting nonlinear manoeuvring models. The result shows that identification of the uncertain parameters using the truncated singular values decomposition and Tikhonov regularization resulted in good estimating the parameters and significantly diminish the uncertainty.

Keywords: Parameter uncertainty; Tikhonov regularization; Truncated singular values decomposition; Nonlinear Lagrangian Manoeuvring Model; Planar Motion Mechanism test.

NOMENCLATURE

$\boldsymbol{v_1}$	Linear velocity of the rigid body, expressed in Body-fixed frame
$\boldsymbol{v_2}$	Angular velocity of the rigid body, expressed in Body-fixed frame
$\boldsymbol{M}_{RB}$	Rigid-body mass matrix
$\boldsymbol{T}$	Kinetic energy of the rigid body
$\boldsymbol{S}$	Skew-symmetric cross-product
$\boldsymbol{\tau}$	Hydrodynamic forces and moments
u,v,w	Velocity in surge, sway and heave
p,q,r	Angular velocity of roll, pitch and yaw
X,Y,Z	Forces of surge, sway and heave
K,M,N	Moments of roll, pitch and yaw
$\boldsymbol{C}_{RB}$	Rigid-body Coriolis-centripetal matrix
$\boldsymbol{M}_A$	Added mass matrix
$\boldsymbol{C}_A$	Added Coriolis-centripetal matrix
$D(\boldsymbol{v})$	Nonlinear damping matrix
ρ	Water density
L	Ship length
U	Total speed
$X'_{uu}, X'_{uuu} \cdots$	Surge nondimensionalized hydrodynamic coefficients
$Y'_{uv}, Y'_{ur}, \cdots$	Sway nondimensionalized hydrodynamic coefficients
$N'_{uv}, N'_{ur}, \cdots$	Yaw nondimensionalized hydrodynamic coefficients
θ	Hydrodynamic coefficients matrix
$\boldsymbol{X}$	Matrix contains the measured data
$\boldsymbol{\tau}_{RB}$	Hydrodynamic forces and moments
y	Measurement data
$\hat{y}(x,\theta^*)$	Estimation values
$\overline{y}$	Mean value of measurement data
$\chi^2(\theta)$	Chi-squared errors
R^2	The goodness of fit criterion
$\boldsymbol{V}_y$	Diagonal matrix of variances of y
$\boldsymbol{V}_{\hat{\theta}}$	Error propagation matrix.
$\boldsymbol{U}$	Left-singular vectors
$\boldsymbol{V}$	Right-singular vectors
Σ	Singular values matrix
$\boldsymbol{P}, \boldsymbol{Q}$	Weighting matrices
β^2	Tikhonov regularization factor
$\overline{\theta}$	Reference parameter vector
$\boldsymbol{U}_r$	Truncated left-singular vectors
$\boldsymbol{V}_r$	Truncated right-singular vectors
Σ_r	Truncated singular values matrix
$\sigma_{\hat{\theta}}$	Standard error of the parameters

1. Introduction

Mathematical modelling of marine vessels has been drawing more and more attention related to the requirements of marine ship design, and ship manoeuvring and operation. The development of numerical computation makes it possible to simulate the ship response travelling with the complicated environmental disturbance and vessel simulators are playing an important role in the testing and verification of the computer software of the complex system, such as dynamic positioning (DP) ships (Sørensen, 2011), remotely operated vehicles (ROVs) operations and control systems (Moreira and Guedes Soares, 2011; Fernandes et al., 2015; Ridao et al., 2015), and ship simulators (Varela and Guedes Soares, 2015a, 2015b). Many mathematical models of marine vessels have been proposed to meet application requirements, such as Abkowitz model (Abkowitz, 1980), Maneuvering Modeling Group (MMG) model (Yoshimura, 2005), Nomoto model (Nomoto et al., 1956), a core mathematical model for hard manoeuvres (Sutulo and Guedes Soares, 2015; Sutulo and Guedes Soares, 2011), and vectorial model (Fossen, 2011). These models have different features and are proposed for different application purposes considering the trade-off between the complexity and fidelity. For example, Nomoto model was proposed for autopilot design only considering the yaw motion. The vectorial model proposed by Fossen (2011) is describing the motion of ships in a vectorial setting. Vectorial models are extensively used in the stability analysis and designing controllers and observers for marine ships. The model of Sutulo and Guedes Soares (2015; 2011) allows describing arbitrary 3DOF ship manoeuvring motions.

Estimation of the hydrodynamic coefficients is a challenge and an interesting topic (ITTC, 2002). Captive model test carried out in a multi-purpose towing tank (SINTEF), is a reliable and effective method to measure the hydrodynamic forces and moments from which hydrodynamic coefficients in manoeuvring model can be determined (Sutulo and Guedes Soares, 2006). System identification is a mature technique for building mathematical models of dynamical systems from measured data (Ljung, 1999). Now it has been widely used for estimation the hydrodynamics coefficients for marine vessels (Åström and Källström, 1976; Golding et al., 2006; Perera, et al, 2012; Luo et al., 2014; Luo and Zou, 2009; Ross et al., 2015; Sutulo and Guedes Soares, 2014; van de Ven et al., 2007; Xu et al., 2018c). Many methods have been developed for system identification, and Least Squares (LS) is one of the most popular methods. In (Golding et al., 2006), the nonlinear viscous damping forces of a surface vessel in the horizontal plane was estimated using the Least Squares method. In (Ross et al., 2015), the Least Squares method was used to estimate the hydrodynamic coefficients based on Planar Motion Mechanism (PMM) tests. The obtained mathematical model was then validated by reproducing the manoeuvring test conducted in full-scale (Hassani et al., 2015). In (Sutulo and Guedes Soares, 2015; Sutulo and Guedes Soares, 2014), an optimal offline system identification method combined the Least Squares with genetic algorithm was proposed to estimate the parameters of a nonlinear manoeuvring mathematical model.

Other methods have been employed to estimate the hydrodynamic coefficients. For example, van de Ven et al., (2007), used a neural network to estimate the damping matrix of an underwater vehicle. Moreira and Guedes Soares, (2003) adopted recursive neural networks for a dynamic model of manoeuvrability. Extended Kalman filter (EKF) is also a good option and it was used for parameter estimation. Fossen et al. (1996) proposed an off-line parallel extended Kalman filter algorithm utilizing two measurement series in parallel to estimate the parameters of the dynamic positioning ship model. An adaptive wave filter coupled with a maximum likelihood parameter identification technique was proposed by Hassani et al. (2013) and used for dynamic positioning control of marine vessels. In (Perera et al., 2016, 2015), the parameters of a modified Nomoto model for vessel steering were identified using an extended Kalman filter.

Recently, the support vector machine (SVM) has been applied to estimate the hydrodynamic coefficients of a ship model (Luo and Zou, 2009; Luo et al., 2016). SVM is a supervised machine learning algorithm, which can be used for both classifications (Suykens and Vandewalle, 1999) or regression challenges (Cortes and Vapnik, 1995; Suykens et al., 2002). It has been receiving much attention in the last decade and was one of the most popular machine learning algorithms. In (Hou et al., 2018), a roll motion equation for floating structures in irregular waves was identified using a ε support vector regression. A modified version, Least Squares Support Vector Machine (LSSVM) was applied to model the controller of the marine surface vehicle for path following scenarios based on manoeuvring test (Xu and Guedes Soares, 2018a, 2016). An online-version of LSSVM was used for dynamic ship steering modelling based on free-running model tests (Xu et al., 2018b).

Least Squares is a simple and popular method for parameter estimation, but there are also some disadvantages (Chen and Ljung, 2013; Ljung, 1999). The parameters estimated by Least Squares method are usually largely affected by the noise of training data and it usually leads to non-consistent estimates (Söderström, 2013). Truncated singular value decomposition (TSVD) (Golub and Reinsch, 1970) is a good option to solve the ill-conditioned problem of the Least Squares method (Chan and Hansen, 1990). The main assumption is to neglect its smallest singular values (Hansen, 1998) because the data corresponding to smaller singular values usually imposes more uncertainty in the process of estimating uncertain parameters. Liu et. al. (2017) proposed a novel method to establish a model, which can efficiently reduce the ill-posedness combining with the singular value decomposition. In (Chen and Ljung, 2013), a regularized least-square method was used to solve the hyper-parameter estimation problem with large data sets and ill-conditioned computations. Tikhonov regularization (Bell et al., 1978) is the most commonly used method of regularization of ill-posed problems. It can significantly improve the condition number by modifying the normal equations in the Least Squares method while leaving the estimated parameter relatively unchanged. The effect of Tikhonov regularization is to estimate the parameters while also keep them near the reference values (Golub et al., 1999; Hansen and O'Leary, 1993; Ma et al., 2017).

The uncertainty of the identified parameters due to the ill-conditioned problem is also a challenge problem in marine ship modelling. The obtained parameters with a large uncertainty are very sensitive to the noise in the measured data and usually drift from the true values, which was called parameter drift (Hwang, 1980; Liu et al., 2016). In (Hwang, 1980), the dynamic cancellation was found and the linear hydrodynamic coefficients drift simultaneously using slender-body theory. In (Luo and Li, 2017), nonlinear hydrodynamic coefficients was also found due to the so-called multicollinearity. The parameter drift cannot be eliminated due to physical reasons, and several methods were proposed in (Hwang, 1980; Luo and Li, 2017) to diminish the parameters drift, such as parallel processing and additional excitation. It is necessary to point that the main purpose of these methods is to reconstruct the samples and improve the condition number.

The main contribution of this paper is to give a mathematical explanation for the parameter drift and two methods, truncated singular values decomposition and Tikhonov regularization, are introduced to diminish the uncertainty of the hydrodynamic coefficients due to the noise in the measured data. A nonlinear manoeuvring mathematical model of a marine surface ship in 3 degrees of freedom (DOF) is derived using

Lagrange's method. In order to compare the coefficients of different ships, the hydrodynamic coefficients have been converted to the dimensionless ones using the prime system of SNAME (SNAME, 1950). The identification procedure uses a data set from a series of PMM tests, carried out by SINTEF Ocean (Ocean) on their multi-purpose towing tank (SINTEF) using a scaled ship model of research vessel Gunnerus (Hassani et al., 2015). Various captive model tests recommended by ITTC (2002) have been carried out, such as pure sway, pure yaw and mixed sway and yaw. The nondimensionalized hydrodynamic coefficients are obtained using the classical Least Square, TSVD, and Tikhonov regularization. The resulted nonlinear manoeuvring models were further tested against the portion of the data that was not used in the identification process. The R^2 goodness of fit criterion is used to demonstrate the accuracy of the obtained models. Uncertainty analysis of the obtained hydrodynamic coefficients is carried out. The results show that TSVD and Tikhonov regularization can provide more stable results and diminish the parameter drift.

The rest paper is organized as follows. In section 2, a nonlinear manoeuvring modelling in 3-DOFs is derived using Lagrange's method, and dimensionless form is given using the prime system of SNAME. In section 3, uncertainty analysis of the identified parameters is given using singular value decomposition. In order to diminish the parameter uncertainty, the Least Squares and Tikhonov regularization combined with the singular value decomposition are presented in section 4. Section 5 describes the planar motion mechanism (PMM) Tests. In section 6, validation and uncertainty analysis of the obtained hydrodynamic coefficients using PMM test data are presented. The final section is the conclusion.

2. Nonlinear Manoeuvring modelling using Lagrange's method

The Newton's Second Law is one of the widely used methods for the mathematical modelling of a rigid body motion, but the disadvantage is that it describes the motion in an inertial reference frame and difficult to switch to a different coordinate system. The Lagrangian method, in contrast, is independent of the coordinates (Lurie, 2002). In this section, the manoeuvring model for a marine ship is derived using Kirchhoff's equations (Kirchhoff, 1869). Consider a ship with linear velocity $\boldsymbol{v}_1 = [u, v, w]^T$ and angular velocity $\boldsymbol{v}_2 = [p, q, r]^T$, The Kirchhoff's equations is given (Fossen, 2011):

$$\underbrace{\frac{d}{dt}(\frac{\partial T}{\partial \boldsymbol{v}_1})}_{mass-terms}+\underbrace{\boldsymbol{S}(\boldsymbol{v}_2)\frac{\partial T}{\partial \boldsymbol{v}_1}}_{Coriolis-centrip}=\boldsymbol{\tau}_1$$
$$\underbrace{\frac{d}{dt}(\frac{\partial T}{\partial \boldsymbol{v}_2})}_{mass-terms}+\underbrace{\boldsymbol{S}(\boldsymbol{v}_2)\frac{\partial T}{\partial \boldsymbol{v}_2}+\boldsymbol{S}(\boldsymbol{v}_1)\frac{\partial T}{\partial \boldsymbol{v}_1}}_{Coriolis-centripetal\ moments}=\boldsymbol{\tau}_2 \quad (1)$$

where $T=\frac{1}{2}\boldsymbol{v}^T\boldsymbol{M}_{RB\_6DOF}\boldsymbol{v}$ is the kinetic energy of the rigid body; $\boldsymbol{S}$ is the skew-symmetric cross-product operator; $\boldsymbol{\tau}$ represents the forces and moment, $\boldsymbol{\tau}_1=[X,Y,Z]^T$ and $\boldsymbol{\tau}_2=[K,M,N]^T$. For convenience, we assumed that the equations are solved at the centre of gravity and the ship is port-starboard symmetric. The mass matrix in 6 degrees of freedom (DOF) can be formed as:

$$\boldsymbol{M}_{RB\_6DOF}=\begin{bmatrix} m & 0 & 0 & 0 & 0 & 0 \\ 0 & m & 0 & 0 & 0 & 0 \\ 0 & 0 & m & 0 & 0 & 0 \\ 0 & 0 & 0 & I_x & 0 & I_{xz} \\ 0 & 0 & 0 & 0 & I_y & 0 \\ 0 & 0 & 0 & I_{xz} & 0 & I_z \end{bmatrix}. \quad (2)$$

Then the Kirchhoff's equations (Eq. 1) can be solved as:

$$\frac{d}{dt}(\frac{\partial T}{\partial \boldsymbol{v}_1})+\boldsymbol{S}(\boldsymbol{v}_2)\frac{\partial T}{\partial \boldsymbol{v}_1}=\begin{bmatrix} m\dot{u}-mvr+mqw \\ m\dot{v}+mur-mpw \\ m\dot{w}-muq+mvp \end{bmatrix} \quad (3)$$

$$\frac{d}{dt}\left(\frac{\partial T}{\partial \boldsymbol{v}_2}\right)+\boldsymbol{S}(\boldsymbol{v}_2)\left(\frac{\partial T}{\partial \boldsymbol{v}_2}\right)+\boldsymbol{S}(\boldsymbol{v}_1)\left(\frac{\partial T}{\partial \boldsymbol{v}_1}\right)=\begin{bmatrix} I_x\dot{p}+\left(I_z-I_y\right)qr+I_{xz}pq \\ I_y\dot{q}\left(I_x-I_z\right)pr-I_{xz}\left(p^2+r^2\right) \\ I_z\dot{r}+\left(I_y-I_z\right)pq-I_{xz}qr \end{bmatrix} \quad (4)$$

For ship manoeuvring study, the 3 degrees of freedom (DOFs), surge, sway and yaw motion, are usually considered (Sutulo and Guedes Soares, 2011). The above equations are rewritten in a vectorial setting with emphasis placed on matrix properties like positiveness, symmetry and skew-symmetry(Berge and Fossen, 2000). Those properties benefit the marine control system design (controller and observer) (Fossen, 2011). So, the above equations can be formulated into:

$$\boldsymbol{M}_{RB}\dot{\boldsymbol{v}} + \boldsymbol{C}_{RB}(\boldsymbol{v})\boldsymbol{v} = \boldsymbol{\tau}_{RB}, \quad (5)$$

where $\boldsymbol{M}_{RB}$ is the mass matrix in 3 DOF (surge, sway and yaw), it is same as derived using Newton's Second Law. $\boldsymbol{C}_{RB}$ is the rigid body Coriolis-centripetal matrix, and it can be considered to be a correction of the first to compensate for the fact that the equation is being solved in a non-inertial frame of reference (Fossen, 2011; Ross, 2008).

$$\boldsymbol{M}_{RB} = \begin{bmatrix} m & 0 & 0 \\ 0 & m & 0 \\ 0 & 0 & I_z \end{bmatrix}, \quad (6)$$

$$\boldsymbol{C}_{RB} = \begin{bmatrix} 0 & 0 & -mv \\ 0 & 0 & mu \\ mv & -mu & 0 \end{bmatrix}, (7)$$

$$\boldsymbol{\tau}_{RB} = [X, Y, N]^T. \quad (8)$$

When a ship moving through water, the kinetic energy is imparted to the fluid. These forces due to the water around the ship are usually proportioned to the acceleration of the ship. So they are denoted as added-mass, represented as in (Fossen, 2011):

$$\boldsymbol{M}_A = \begin{bmatrix} X_{\dot{u}} & 0 & 0 \\ 0 & Y_{\dot{v}} & Y_{\dot{r}} \\ 0 & N_{\dot{v}} & N_{\dot{r}} \end{bmatrix}, \quad (9)$$

where, $X_{\dot{u}}$ and $Y_{\dot{v}}$ are the added-mass in surge and sway motion, respectively. $N_{\dot{r}}$ is the add-inertia moment. $Y_{\dot{r}}$ and $N_{\dot{v}}$ are the cross-inertia terms.

Then the kinetic energy is given:

$$T_A = \frac{1}{2}\boldsymbol{v}^T \boldsymbol{M}_A \boldsymbol{v} = \frac{1}{2}\boldsymbol{v}^T \bar{\boldsymbol{M}}_A \boldsymbol{v}\,, \quad (10)$$

where $\bar{\boldsymbol{M}}_A = \frac{1}{2}\left(\boldsymbol{M}_A + \left(\boldsymbol{M}_A\right)^T\right)$ is the symmetric part of $\boldsymbol{M}_A$. The skew-symmetric parts can have no influence whatsoever on the kinetic energy of the system (Fossen, 2011). Applying the Kirchhoff's equations, then the forces on the rigid body due to added-mass can get:

$$\begin{aligned}
X_A &= -\frac{d}{dt}\left(\frac{\partial T_A}{\partial u}\right) + r\frac{\partial T_A}{\partial v} \\
Y_A &= -\frac{d}{dt}\left(\frac{\partial T_A}{\partial v}\right) - r\frac{\partial T_A}{\partial u} \\
N_A &= \underbrace{-\frac{d}{dt}\left(\frac{\partial T_A}{\partial r}\right)}_{Added\ mass} \underbrace{+ v\frac{\partial T_A}{\partial u} - u\frac{\partial T_A}{\partial v}}_{Coriolis-centripetal}
\end{aligned} \quad (11)$$

Then the Coriolis-centripetal forces in the matrix can be expressed as (Fossen, 2011):

$$\boldsymbol{C}_A(\boldsymbol{v})\boldsymbol{v} = \begin{bmatrix} 0 & 0 & Y_{\dot{v}}\, v + Y_{\dot{r}}\, r \\ 0 & 0 & -X_{\dot{u}} u \\ -Y_{\dot{v}}\, v - Y_{\dot{r}}\, r & X_{\dot{u}} u & 0 \end{bmatrix} \cdot \begin{bmatrix} u \\ v \\ r \end{bmatrix} \quad (12)$$

Hydrodynamic damping forces are very complex and mainly caused by lift and drag, cross-flow drag, vortex shedding el. al (Fossen, 2011). It constitutes the most awkward and ill-defined of the forces and moments acting on a ship. Here, the structure of nonlinear damping forces is adopted from the reference (Ross, 2008; Ross et al., 2007), where the total damping forces are derived into two terms, damping due to lift and drag and crossflow drag. The total damping matrix is given:

$$
D(\boldsymbol{v}) = \begin{bmatrix} \begin{matrix} -X_{uu}u - X_{uu}u^2 \\ -X_{uvr}vr - X_{u|v|}|v| \end{matrix} & \begin{matrix} -X_{vv}v - X_{rv}r \\ -X_{uvv}uv \end{matrix} & -X_{rr}r - X_{urr}ur \\ 0 & \begin{matrix} -Y_{uv}u - Y_{uuv}u^2 - Y_{vvv}v^2 \\ -Y_{rrv}r^2 - Y_{|v|v}|v| - Y_{|r|v}|r| \end{matrix} & \begin{matrix} -Y_{ur}u - Y_{uur}u^2 - Y_{rrr}r^2 \\ -Y_{vvr}v^2 - Y_{|v|r}|v| - Y_{|r|r}|r| \end{matrix} \\ 0 & \begin{matrix} -N_{uv}u - N_{uuv}u^2 - N_{vvv}v^2 \\ -N_{rrv}r^2 - N_{|v|v}|v| - N_{|r|v}|r| \end{matrix} & \begin{matrix} -N_{ur}u - N_{uur}u^2 - N_{rrr}r^2 \\ -N_{vvr}v^2 - N_{|v|r}|v| - N_{|r|r}|r| \end{matrix} \end{bmatrix}, \quad (13)
$$

where $X_{uu}, \cdots, N_{|r|r}$ are the hydrodynamic coefficients (or regression coefficients), which are supposed to be identified and constant for a manoeuvering model.

The forces in the 3DOF nonlinear manoeuvring model described in Eq. 5 can be written as:

$$
\boldsymbol{\tau}_{RB} = -\boldsymbol{M}_A\dot{\boldsymbol{v}} - \boldsymbol{C}_A(\boldsymbol{v}_r)\boldsymbol{v}_r - \boldsymbol{D}(\boldsymbol{v}_r)\boldsymbol{v}_r \,. \qquad (14)
$$

The equations of the hydrodynamic forces and moment can be expressed as follow:

$$
\begin{aligned} X &= X_{\dot{u}}\dot{u} + Y_{\dot{v}}\,vr + Y_{\dot{r}}\,rr + X_{uu}uu + X_{uuu}uuu \\ &+ X_{rvu}rvu + X_{vv}vv + X_{rv}rv + X_{uvv}uvv + X_{rr}rr \\ &+ X_{urr}urr + X_{u|v|}u|v| \end{aligned} \qquad (15)
$$

$$
\begin{aligned} Y &= Y_{\dot{v}}\,\dot{v} + Y_{\dot{r}}\,\dot{r} + X_{\dot{u}}ur + Y_{uv}uv + Y_{ur}ur + Y_{uur}uur \\ &+ Y_{uuv}uuv + Y_{vvv}vvv + Y_{rrr}rrr + Y_{rrv}rrv + Y_{vvr}vvr \\ &+ Y_{v|r|}v|r| + Y_{v|v|}v|v| + Y_{r|v|}r|v| + Y_{r|r|}r|r| \end{aligned} \qquad (16)
$$

$$
\begin{aligned} N &= N_{\dot{v}}\dot{v} + N_{\dot{r}}\dot{r} + (Y_{\dot{v}} - X_{\dot{u}})vu + Y_{\dot{r}}\,ur \\ &+ N_{uv}uv + N_{ur}ur + N_{uur}uur + N_{uuv}uuv + N_{vvv}vvv \\ &+ N_{rrr}rrr + N_{rrv}rrv + N_{vvr}vvr + N_{v|r|}v|r| \\ &+ N_{v|v|}v|v| + N_{r|v|}r|v| + N_{r|r|}r|r| \end{aligned} \qquad (17)
$$

In order to compare the coefficients of different ships and to estimate the dynamics of a full-size ship, the hydrodynamic parameters need to be converted to dimensionless ones. The most commonly used normalization forms for the manoeuvring of the marine ship is the prime system of SNAME (SNAME, 1950). The water density, ρ , the ship length L and the ship speed U are employed as the characteristic dimensional parameter. The list of the nondimensionalized factors and corresponding coefficients in Eqs. (14)-(16) is shown in Table 1.

Table 1. Dimensional factors for nondimensionalized the hydrodynamic coefficients.

Coef.	Dimensional Factor	Coef.	Dimensional Factor	Coef.	Dimensional Factor
$X_{\dot{u}}^{0}$	$0.5\rho L^3$	$Y'_{\dot{v}}$	$0.5\rho L^3$	$N'_{\dot{v}}$	$0.5\rho L^4$
X'_{uu}	$0.5\rho L^2$	$Y'_{\dot{r}}$	$0.5\rho L^4$	$N'_{\dot{r}}$	$0.5\rho L^5$
X'_{uuu}	$0.5\rho L^2 U^{-1}$	Y'_{uv}	$0.5\rho L^2$	N'_{uv}	$0.5\rho L^3$
X'_{rvu}	$0.5\rho L^3 U^{-1}$	Y'_{ur}	$0.5\rho L^3$	N'_{ur}	$0.5\rho L^4$
X'_{vv}	$0.5\rho L^2$	Y'_{uur}	$0.5\rho L^3 U^{-1}$	N'_{uur}	$0.5\rho L^4 U^{-1}$
X'_{rv}	$0.5\rho L^3$	Y'_{uuv}	$0.5\rho L^2 U^{-1}$	N'_{uuv}	$0.5\rho L^3 U^{-1}$
X'_{uvv}	$0.5\rho L^2 U^{-1}$	Y'_{vvv}	$0.5\rho L^2 U^{-1}$	N'_{vvv}	$0.5\rho L^3 U^{-1}$
X'_{rr}	$0.5\rho L^4$	Y'_{rrr}	$0.5\rho L^5 U^{-1}$	N'_{rrr}	$0.5\rho L^6 U^{-1}$
X'_{urr}	$0.5\rho L^4 U^{-1}$	Y'_{rrv}	$0.5\rho L^4 U^{-1}$	N'_{rrv}	$0.5\rho L^5 U^{-1}$
$X'_{u\|v\|}$	$0.5\rho L^2$	Y'_{vvr}	$0.5\rho L^3 U^{-1}$	N'_{vvr}	$0.5\rho L^3 U^{-1}$
		$Y'_{v\|r\|}$	$0.5\rho L^3$	$N'_{v\|r\|}$	$0.5\rho L^4$
		$Y'_{v\|v\|}$	$0.5\rho L^2$	$N'_{v\|v\|}$	$0.5\rho L^3$
		$Y'_{r\|v\|}$	$0.5\rho L^3$	$N'_{r\|v\|}$	$0.5\rho L^4$
		$Y'_{r\|r\|}$	$0.5\rho L^4$	$N'_{r\|r\|}$	$0.5\rho L^5$

3. Uncertainty analysis of the estimated hydrodynamic coefficients

The uncertainty of the estimated hydrodynamic coefficients due to the noise is discussed in this section. The parameter with a large uncertainty is very sensitive to the noise and usually drift from the true value. This phenomenon was observed by Hwang (Hwang, 1980) and was called parameter drift. The physical reason for the parameter drift was discussed by Hwang using slender-body theory and the multicollinearity was considered as the main factor (Hwang, 1980; Luo, 2016; Luo and Li, 2017). In this section, the classical parameters estimation method, Least Squares (LS), is briefly introduced, and a mathematical explanation of the parameter drift is discussed using singular value decomposition. The above Eqs. (15) to (17) need to be reordered in a vector format given by:

$$\boldsymbol{X}\theta = y, \tag{18}$$

where the matrix $\boldsymbol{X} \in \mathbb{R}^{n*38}$ contains the measured data, $\theta \in \mathbb{R}^{38*1}$ represents the uncertain parameters described in Eq. (19), and $y = [X, Y, N]^T$ is the matrix of the recorded forces and moments during the tests. In this study, there are 38 parameters to be estimated. Obviously, the linear equation is over-determined (n>m).

$$\begin{aligned}\theta = [&X'_{\dot{u}}, Y'_{\dot{v}}, Y'_{\dot{r}}, N'_{\dot{v}}, N'_{\dot{r}}, X'_{uu}, X'_{uuu}, X'_{rvu}, X'_{vv}, X'_{rv}, X'_{uvv}, X'_{rr},\\ &X'_{urr}, X'_{u|v|}, Y'_{uv}, Y'_{ur}, Y'_{uur}, Y'_{uuv}, Y'_{vvv}, Y'_{rrr}, Y'_{rrv}, Y'_{vvr},\\ &Y'_{v|r|}, Y'_{v|v|}, Y'_{r|v|}, Y'_{r|r|}, N'_{uv}, N'_{ur}, N'_{uur}, N'_{uuv}, N'_{vvv},\\ &N'_{rrr}, N'_{rrv}, N'_{vvr}, N'_{v|r|}, N'_{v|v|}, N'_{r|v|}, N'_{r|r|}]\end{aligned} \tag{19}$$

3.1 Parameter estimation using Least Squares method

Considering Eq. (18), the estimation problem is to find the optimal parameters, θ, which can minimise the difference between the estimated values $\hat{y}(x;\theta)$ and the measured data y. In addition, several assumptions need to be made. The first assumption is that the sample of measurements, y_i, are uncorrelated. It is reasonable because each measurement is independent. Each measurement y_i has a particular variance, σ_y^2, due to the environmental disturbance and sensors.

In order to find the optimal parameters, the residual error, $e = \hat{y}(x_i;\theta) - y$, need to be defined first. Furthermore, the error needs to be dominated by the high-accuracy data (small-variance) and less affected by the low-accuracy data (large-variance). So the weighted sum of the squared residuals, also called *'chi-squared'* is defined in terms of the vectors:

$$\chi^2(\theta) = (\boldsymbol{X}\theta - y)^T \boldsymbol{V}_y^{-1} (\boldsymbol{X}\theta - y), \tag{20}$$

where $\boldsymbol{V}_y$ is the diagonal matrix of variances of y. Usually, it can be assumed to be the identity matrix if the variances of y is unknown in advance. The optimal parameters, θ, corresponds to the minimum value of the χ^2 error function, which means the derivative of χ^2 respect to the θ equals to zero.

$$\left.\frac{\partial \chi^2}{\partial \theta}\right|_{\theta=\hat{\theta}} = 0 \qquad (21)$$
$$\boldsymbol{X}^T \boldsymbol{V}_y^{-1} \boldsymbol{X}\hat{\theta} - \boldsymbol{X}^T \boldsymbol{V}_y^{-1} y = 0$$

Then the optimal values of the parameters can be obtained as

$$\hat{\theta} = [\boldsymbol{X}^T \boldsymbol{V}_y^{-1} \boldsymbol{X}]^{-1} \boldsymbol{X}^T \boldsymbol{V}_y^{-1} y\,. \qquad (22)$$

The χ^2 error function can be minimized with respect to the parameters θ. The estimated values, which have the best agreement with the measured data, can be computed using $\hat{y}(x_i;\hat{\theta}) = \boldsymbol{X}\hat{\theta}$.

3.2 Uncertainty analysis due to the ill-conditioned matrix

The uncertainty analysis of the identified parameters in the model is of paramount importance to obtain a robust model. Large uncertainty or covariance of the parameters can be due to noise in data or an ill-conditioned model (or both). If the obtained parameters with a large uncertainty, it means that the parameters drift from their true values with higher probability. A poorly identified model (models with large parametric uncertainty) is very sensitive to the disturbance in the input data. Such a model cannot reproduce the behaviour of the system with high accuracy. This is due to the fact that the parameters with large uncertainty will change dramatically with the errors in the measured data. In this section, singular value decomposition is introduced to analysis the uncertainty of the hydrodynamic coefficients due to the noise in data. The matrix $\boldsymbol{X}$ can be rewritten as

$$\boldsymbol{X} = \sum_{i=1}^{n} u_i \sigma_i v_i^T = \boldsymbol{U}\Sigma\boldsymbol{V}^T\,, \qquad (23)$$

where the matrix $\boldsymbol{U}$ and $\boldsymbol{V}$ are orthonormal, $\boldsymbol{U}^T\boldsymbol{U} = \boldsymbol{I}$ and $\boldsymbol{V}^T\boldsymbol{V} = \boldsymbol{I}$. Σ is the diagonal matrix of the singular values of the matrix $\boldsymbol{X}$. Furthermore, substitution of Eq. (23) into the optimal parameter estimation in Eq. (18) gives:

$$\theta = \boldsymbol{V}\Sigma^{-1}\boldsymbol{U}^T y = \sum_{i=1}^{n} \frac{v_i u_i^T y}{\sigma_i} . \qquad (24)$$

As presented in Eq. (24), the smaller singular values can potentially dominate the solutions θ. Assume that there is an additive perturbation, δy , it will propagate to a perturbation in the solution,

$$\delta\theta = \boldsymbol{V}\Sigma^{-1}\boldsymbol{U}^T \delta y = \sum_{i=1}^{n} \frac{v_i u_i^T}{\sigma_i} \delta y . \qquad (25)$$

The smaller the singular value σ_i is, the more uncertainty the estimated parameters have. For example, if σ_i is close to the numerical precision of the computation, then the singular values σ_i and the corresponding columns of $\boldsymbol{U}$ and $\boldsymbol{V}$ contribute negligibly to the matrix $\boldsymbol{X}$. Their contribution to the solution can be easily dominated by the noise and round-off error in the recorded data (y). The condition number is usually used to measure how sensitive the matrix $\boldsymbol{X}$ is to the error the recorded data (y). If the condition number is large, then it is ill-conditioned. The condition number for Eqs. (15)-(17) is given in Table 2.

Table 2: The condition number of the surge, sway and yaw motion

	Surge	Sway	Yaw
Condition number	2.77e+19	4.33e+16	2.81e+18

The uncertainty of parameters is affected by noise and quantified by the error propagation matrix. The error propagation matrix or covariance matrix can be used to indicate how the random errors in the recorded data (y), as described by $\boldsymbol{V}_y$, propagate to the optimal parameter $\hat{\theta}$. The error propagation matrix is given by

$$\boldsymbol{V}_{\hat{\theta}} = \left[\frac{\partial\hat{\theta}}{\partial y}\right] \boldsymbol{V}_y \left[\frac{\partial\hat{\theta}}{\partial y}\right]^T \qquad (26)$$

where the standard error of the parameters, $\sigma_{\hat{\theta}}$, can get by calculation of the square-root of the diagonal of the error propagation matrix. Then the absolute error can be calculated easily. The confidence intervals for the parameters can get by:

$$\hat{\theta} - t_{1-\alpha/2}\sigma_{\hat{\theta}} \leq \theta \leq \hat{\theta} + t_{1-\alpha/2}\sigma_{\hat{\theta}} \qquad (27)$$

where $1-\alpha$ is the desired confidence level, and *t* is the Student-*t* statistic.

4. The methods for diminishing the parameter uncertainty

In this section, in order to alleviate or diminish the uncertainty, two methods, truncated singular value decomposition (TSVD) and Tikhonov regularization, are introduced to estimate the parameters.

4.1 Optimal truncated singular value decomposition

In order to get a physically meaningful solution, it is necessary to reduce the effect caused by the smaller singular values. In most cases, TSVD is an effective tool to reduce the uncertainty of the data set. TSVD is used to obtain a relatively accurate representation of the matrix $\boldsymbol{X}$ by simply retaining the first r singular values of $\boldsymbol{X}$ and the corresponding columns of $\boldsymbol{U}$ and $\boldsymbol{V}$. The TSVD can be presented as

$$\boldsymbol{X}_r = \boldsymbol{U}_r \boldsymbol{\Sigma}_r \boldsymbol{V}_r^T , \qquad (28)$$

where the matrix $\boldsymbol{\Sigma}_r$ is obtained by retaining the first *r* singular values of $\boldsymbol{\Sigma}$. Similarly, matrices $\boldsymbol{U}_r$ and $\boldsymbol{V}_r$ are found using the corresponding singular vectors. The resulting $\boldsymbol{X}_r$ represents the reduced data set where the data related to the omitted singular values are filtered.

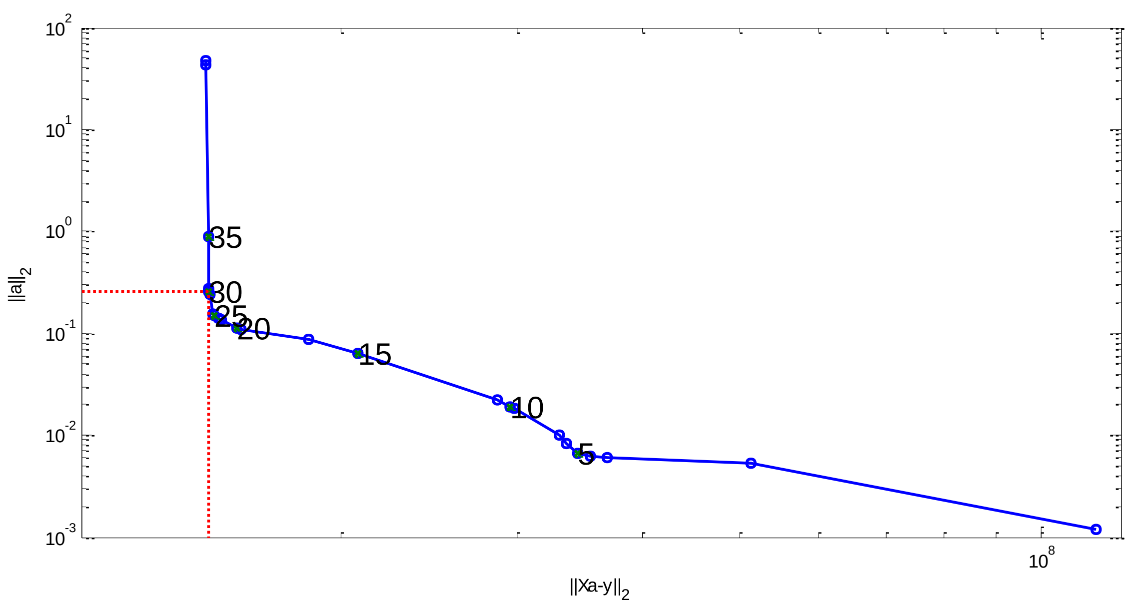

Fig. 1: Estimate the optimal values of *r* using *L-Curve*

It should be noted that truncation of the original matrix will inevitably increase the bias error for the parameters due to the loss of some information, but the uncertainty of the parameters (parameters drift) can be reduced significantly. As presented in the following section, the bias error for the parameters increases slightly, because the smaller singular values contribute little to the parameters. The optimal value of r can be estimated using the *L-curve*. It is a log-log plot of the norm of a regularized solution versus the norm of the corresponding residual norm. It is a convenient graphical tool for displaying the trade-off between the size of a regularized solution and its fit to the given data, as the regularization parameter varies (Golub et al., 1999; Hansen and Johnston, 2001; Hansen and O'Leary, 1993). As presented in Fig. 1 in our current data set the optimal r equals to 30.

4.2 Tikhonov regularization with singular value decomposition

Tikhonov regularization is the most commonly used method of regularization of ill-posed problems (Bell et al., 1978). The goal of regularization is to improve the condition number of the matrix $\boldsymbol{X}$ while leaving the solution relatively unchanged. The effect of Tikhonov regularization is to estimate model parameters while also keeping the model parameters near some reference values. In Tikhonov regularization, a quadratic term involving the parameters, θ, is included in the Least Squares error function. Consider Eq. (18), the cost function for Tikhonov regularization can be defined as:

$$J(\theta) = \left\| \boldsymbol{X}\theta - y \right\|_P^2 + \beta^2 \left\| \theta - \bar{\theta} \right\|_Q^2 \tag{29}$$

where P and Q are the weighting matrices and positively defined. Tikhonov regularization factor, β^2, is non-negative and weights the relative importance of $\left\| \boldsymbol{X}\theta - y \right\|_P^2$ and $\left\| \theta - \bar{\theta} \right\|_Q^2$. The reference parameter vector, $\bar{\theta}$, reflect the way in which we would like to constrain the parameters.

Setting the derivative of $J(\theta)$ respect to the θ equals to zero, then one gets:

$$\frac{\partial J(\theta)^T}{\partial \theta} = 2\boldsymbol{X}^T \boldsymbol{P}\boldsymbol{X}\theta - 2\boldsymbol{X}^T \boldsymbol{P}y + 2\beta^2 \boldsymbol{Q}\theta - 2\beta^2 \boldsymbol{Q}\bar{\theta} = \boldsymbol{0}\,. \tag{30}$$

Solving for the parameter θ, then:

$$\hat{\theta} = \left[\boldsymbol{X}^T \boldsymbol{P}\boldsymbol{X} + \beta^2 \boldsymbol{Q} \right]^{-1} \left(\boldsymbol{X}^T \boldsymbol{P}y + \beta^2 \boldsymbol{Q}\bar{\theta} \right). \tag{31}$$

In most cases, every measurement, y_i, has the same distribution of measurement errors and the measurement errors are uncorrelated. In order to simplify the problem, the difference between the parameters, $\theta-\bar{\theta}$, are assumed to be equally important. So, the weighting matrix $\boldsymbol{P}$ and $\boldsymbol{Q}$ can be set to the identity matrix. If there is no reference parameter set, it is common to set $\bar{\theta}=0$. Then substitute the singular value decomposition of $\boldsymbol{X}$ into Eq. (31):

$$
\begin{aligned}
\hat{\theta} &= \left[\boldsymbol{V}\Sigma\boldsymbol{U}^T\boldsymbol{U}\Sigma\boldsymbol{V}^T+\beta^2 I\right]^{-1}\boldsymbol{V}\Sigma\boldsymbol{U}^T y \\
&= \boldsymbol{V}\left(\Sigma^2+\beta^2 I\right)^{-1}\Sigma\boldsymbol{U}^T y=\sum_{i=1}^{n} v_i\left(\frac{\sigma_i}{\sigma_i^2+\beta^2}\right)u_i^T y
\end{aligned}
\tag{32}
$$

As shown in Eq. (32), the singular values of the matrix $\boldsymbol{X}$ are damped by the Tikhonov regularization factor. It is equivalent to a singular value decomposition solution, in which the inverse of each singular value, $1/\sigma_i$, is replaced by $\sigma_i/\sigma_i^2+\beta^2$. Obviously, the largest singular values are negligibly affected by the regularization factor, but the effects of the smallest singular values on the solution are suppressed.

5. Planar Motion Mechanism (PMM) Tests

A series of captive model tests were carried out by SINTEF Ocean (Ocean) during a research project (SimVal) on the scaled ship model according to the recommended procedures by ITTC (2002). The captive model test is nowadays commonly used to provide data for the identification and validation of mathematical models of ship manoeuvring motion. It can provide a reasonable estimation of the hydrodynamic coefficients, however, performing such tests is costly. In this section, a brief summary of different PMM tests is presented, such as pure surge, pure drift, pure sway, pure yaw and mixed sway and yaw, which were carried out in SINTEF Ocean's multi-purpose towing tank (SINTEF) using the scaled ship model, presented in Fig. 2. The motions in the surge, sway and yaw were controlled using a 6-DOF hexapod motion platform, which is mounted on the carriage. Each type of test emphasises different dynamic characteristics:

Pure Surge: A pure surge test tows the model forward with oscillations around a fixed velocity. It is usually sinusoidal oscillations. This test aims to achieve the full response of surge motion.

Pure Drift: A pure drift test tows the model forward with a fixed oblique angle. This test is usually used to isolate the static derivatives from yaw motion (Ross et al., 2015).

Pure Sway: A pure sway test is used to isolate the sway dynamics from the yaw motion. The ship will move forward with a constant velocity and with a sinusoidal oscillation in sway. This test aims to achieve the full response of sway motion.

Pure Yaw: Similarly, in a pure yaw test, the model will move forward with a sinusoidal oscillation in yaw. The effect of sway can be neglected owing to the zero velocity in sway motion.

Mixed Sway and Yaw: This test was carried out using a ship model at a set of sway velocity and yaw rate. It is a generalization of pure yaw, except the model is held at a nonzero sway (Ross, 2008).

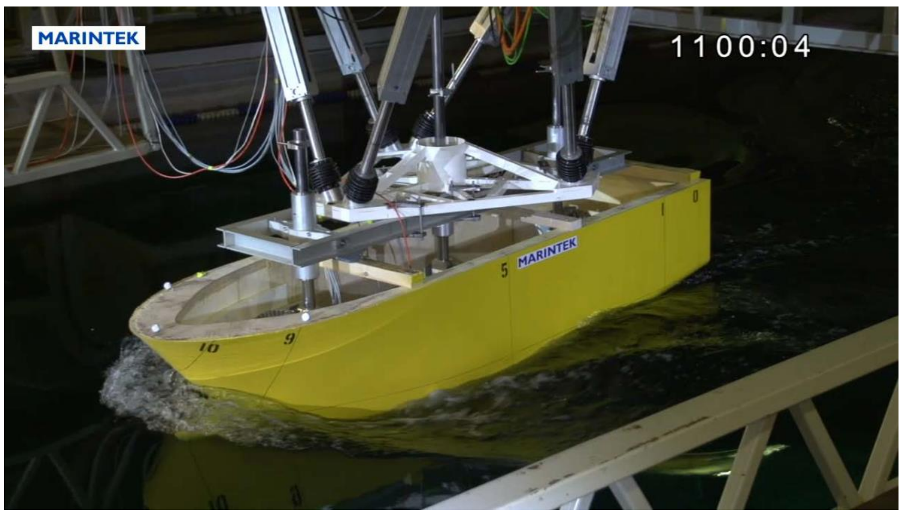

Fig. 2: Planar motion mechanism tests in towing tank [courtesy of SINTEF OCEAN (Ocean)]

6. Validation and Sensitive Analysis of the hydrodynamic Coefficients

In this section, the parameter estimation based on the Least Squares method is presented using the PMM test data. the uncertainty of the obtained hydrodynamic coefficients is discussed. In order to diminish the uncertainty or parameter drift due to the noise, the previously discussed methods truncated singular value decomposition and Tikhonov regularization, are employed to identify the hydrodynamic coefficients. The absolute error of the obtained parameters is compared with results using the Least Squares method. Before the identification process, the data needs to be regrouped to be used as a training set in the identification process. The training set should contain enough information to excite the 3-DOF manoeuvring model (surge, sway and yaw motion). Here, the training set contains data collected from surge acceleration, pure drift, pure surge, pure sway and mixed sway and yaw tests. It is built by simply joining all the data in sequence. A small portion of the data was kept for validation. The same process is carried out to construct a new data set for validation purpose.

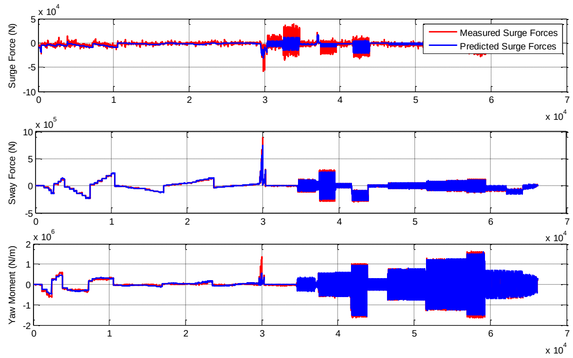

(a)

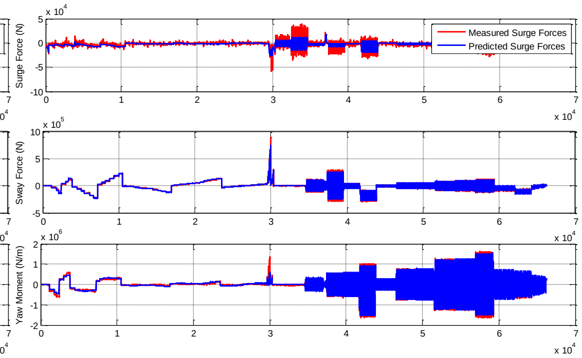

(b)

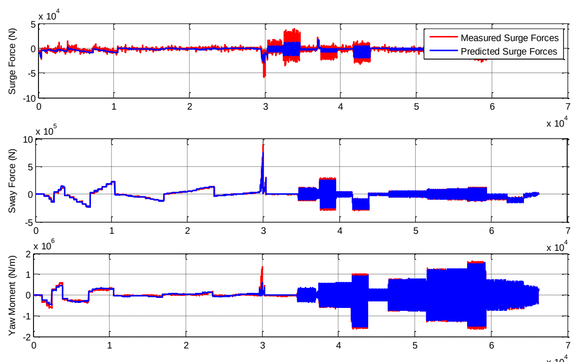

(c)

Fig. 3: The experimental test compares with the prediction of the regressed numerical model obtained by LS (a), TSVD (b) and Tikhonov regularization (c).

In order to assess the performance of the numerical model, the data for validation was not used for training. In the first phase, the parameter estimation based on Least Squares method has been carried out using training set. The prediction of forces and moments compared with training data is presented in Fig. 3(a). From this figure, the curves fit well with each other, especially for sway force and yaw moments. A similar process was also carried out after treating the data set using the TSVD and Tikhonov regularization, as shown in

Fig.3 (b) and (c). Furthermore, the obtained numerical model also can predict the system response successfully.

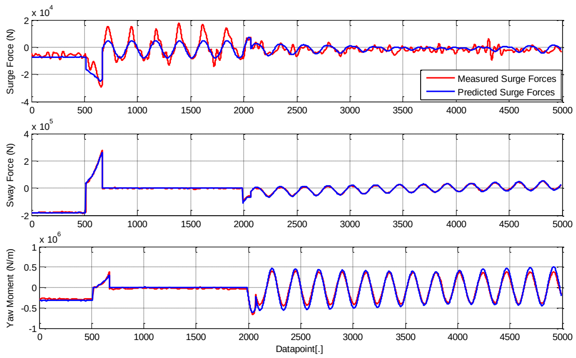

(a)

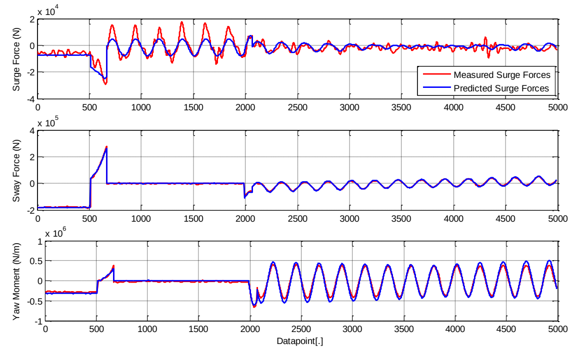

(b)

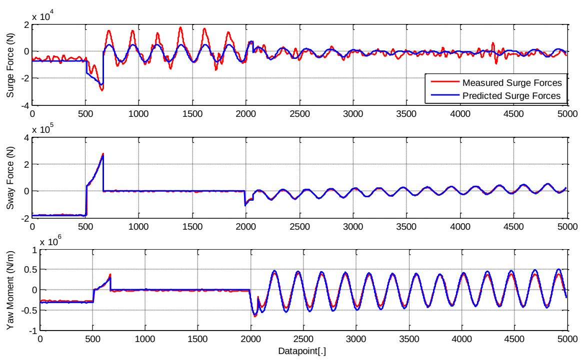

(c)

Fig. 4: Validation of the obtained manoeuvring model obtained by LS (a), TSVD (b) and Tikhonov regularization (c).

Table 3: the R^2 goodness of fit criterion for validation.

Methods	Surge	Sway	Yaw
LS	0.6674	0.9913	0.9190
TSVD	0.6881	0.9971	0.9538
Tik	0.6764	0.9964	0.9537

Table 4: The nondimensionalized hydrodynamic coefficients of the Lagrange’s model using LS, TSVD and Tikhonov regularization.

COEF.	LS	TSVD	TIK.	COEF.	LS	TSVD	TIK.
$X'_{\dot{u}}$	-7.28E-03	-7.40E-03	-7.26E-03	Y'_{rrr}	-4.60E-03	-8.64E-04	-3.15E-03
$Y'_{\dot{v}}$	-3.86E-02	-3.86E-02	-3.86E-02	Y'_{rrv}	-1.32E-02	-9.93E-03	-1.04E-02
$Y'_{\dot{r}}$	-2.83E-04	-2.70E-04	-2.69E-04	Y'_{vvr}	5.70E+00	8.12E-03	-3.87E-02
$N'_{\dot{v}}$	1.80E-03	1.80E-03	1.80E-03	$Y'_{v\|r\|}$	-1.20E-02	-1.33E-02	-1.35E-02
$N'_{\dot{r}}$	-1.18E-03	-1.19E-03	-1.19E-03	$Y'_{v\|v\|}$	-1.62E-01	-1.25E-01	-1.18E-01
X'_{uu}	-5.63E-02	-1.96E-04	-6.61E-03	$Y'_{r\|v\|}$	1.54E-01	2.71E-02	4.38E-02
X'_{uuu}	5.62E-02	7.69E-05	6.47E-03	$Y'_{r\|r\|}$	8.26E-03	1.92E-03	5.35E-03
X'_{rvu}	6.73E-02	2.76E-02	3.58E-02	N'_{uv}	-1.23E-01	-1.28E-01	-1.24E-01
X'_{vv}	9.21E-03	3.15E-04	1.27E-02	N'_{ur}	3.27E+00	3.38E-02	3.52E-02
X'_{rv}	-8.33E-03	2.92E-02	2.14E-02	N'_{uur}	-3.27E+00	-4.23E-02	-4.38E-02
X'_{uvv}	1.07E-02	-3.07E-04	-1.48E-02	N'_{uuv}	1.40E-01	1.45E-01	1.40E-01
X'_{rr}	2.13E-02	-3.07E-04	1.05E-02	N'_{vvv}	-1.90E-02	-1.70E-02	-1.84E-02
X'_{urr}	-2.21E-02	-5.06E-04	-1.13E-02	N'_{rrr}	-6.95E-04	-8.89E-04	-8.91E-04
$X'_{u\|v\|}$	-9.46E-04	-2.50E-03	-1.46E-03	N'_{rrv}	2.58E-03	2.62E-03	2.60E-03
Y'_{uv}	5.34E-01	-2.53E-02	-7.86E-03	N'_{vvr}	-4.24E+01	5.77E-03	-1.54E-02
Y'_{ur}	-1.27E+01	1.56E-02	3.63E-03	$N'_{v\|r\|}$	2.31E-03	2.27E-03	2.28E-03
Y'_{uur}	1.27E+01	1.17E-02	2.22E-02	$N'_{v\|v\|}$	6.34E-02	6.36E-02	6.33E-02
Y'_{uuv}	-5.85E-01	-2.84E-02	-4.70E-02	$N'_{r\|v\|}$	-4.88E-02	-2.19E-02	-2.19E-02
Y'_{vvv}	-1.58E-01	3.22E-02	1.38E-02	$N'_{r\|r\|}$	-5.14E-04	-3.77E-05	-3.41E-05

The performance of both numerical models needs to be verified. The manoeuvring model is validated if the model can approximate the measured force and moments of the validation data set with high accuracy. The validation data set is a small portion of all PMM data and is not used for training purpose. The fit of the models obtained by Least Square, TSVD and Tikhonov regularization is presented in Fig. 4. From the figures, all the models work well and can successfully predict the test data. The R^2 goodness of fit criterion is used to measure the goodness of the fitness. The R^2 is the ratio of the variability in the data that is not explained by the model to the total variability in the data. If R^2 equal to zero, it means that the model fails to explain the measurement variability. Otherwise, if R^2 equal to 1, it means that all the variability of measured data can be fully explained by the model. If R^2 is negative, it means the model can explain the data worse than the mean value. The R^2 for the validation process is presented in Table 3. From this table, the three methods have almost equal accuracy in predicting the test data. However, the uncertainty of the obtained hydrodynamic coefficients can be diminished significantly using the TSVD and Tikhonov regularization method.

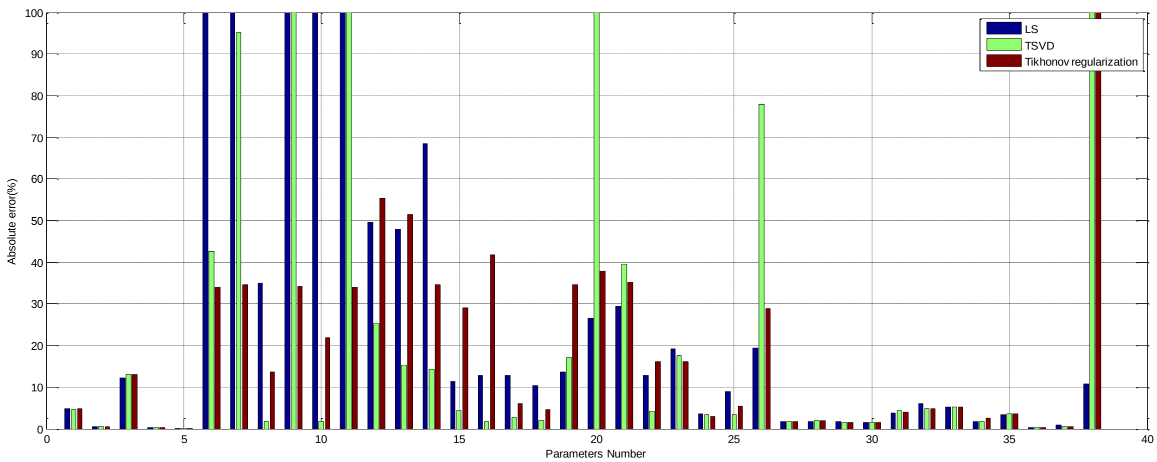

Fig. 5: The uncertainty (absolute error) of the obtained parameters.

The obtained nondimensionalized hydrodynamic coefficients of the Lagrange's model are presented in Table 3. The error propagation matrix of the estimated parameters is calculated using Eq.(25). The absolute errors of the obtained parameters are presented in Table 4. The bar plot is presented in Fig.5. Here, it is assumed that if the absolute error bigger than 100% the obtained parameters are not stable and easily affected by the noise. The identify values will drift from the true value with a large probability. As presented in Fig. 5, there are 5 parameters are failed to be estimated using the Least Squares method, 3 parameters using TSVD and 1 parameters using Tikhonov regularization. Obviously, for example, X_{uu}^{L} and X_{uuu}^{L} are highly linearly correlated, the so-called multicollinearity happens. TSVD and Tikhonov regularization can significantly improve this condition. Observing the absolute errors in Table 4, the proposed methods provide very stable results for the yaw motion equation, the absolute errors are smaller than 6%. It is because that the yaw motion is fully excited using the PMM test. The structure of the yaw motion equation is reasonable. The largest uncertainty occurs in the surge motion because the surging speed is kept as constant during the most PMM test, so the surge motion is not fully excited. For sway motion, the uncertainty is significantly diminished using the TSVD and Tikhonov regularization.

Table 4: The absolute error (%) of the estimated parameters using LS, TSVD and Tikhonov regularization.

NUM.	COEF.	LS	TSVD	TIK.	NUM.	COEF.	LS	TSVD	TIK.
1	$X'_{\dot{u}}$	4.74	4.69	4.78	20	Y'_{rrr}	27	135	37.9
2	$Y'_{\dot{v}}$	0.47	0.48	0.47	21	Y'_{rrv}	29	39	35.2
3	$Y'_{\dot{r}}$	12.24	12.9	12.99	22	Y'_{vvr}	13	4.25	16.2
4	$N'_{\dot{v}}$	0.35	0.35	0.35	23	$Y'_{v\|r\|}$	19	17.54	16.2
5	$N'_{\dot{r}}$	0.10	0.10	0.10	24	$Y'_{v\|v\|}$	3.52	3.36	3.04
6	X'_{uu}	297	42	33.8	25	$Y'_{r\|v\|}$	8.96	3.41	5.50
7	X'_{uuu}	298	95	34.5	26	$Y'_{r\|r\|}$	19.5	78	28.8
8	X'_{rvu}	35	1.73	13.75	27	N'_{uv}	1.73	1.68	1.68
9	X'_{vv}	359	173	34.1	28	N'_{ur}	1.72	1.99	1.90
10	X'_{rv}	267	1.73	21.8	29	N'_{uur}	1.71	1.57	1.52
11	X'_{uvv}	1074	123	34.1	30	N'_{uuv}	1.49	1.45	1.44
12	X'_{rr}	49	25.4	55.2	31	N'_{vvv}	3.90	4.38	3.92
13	X'_{urr}	48	15.4	51.5	32	N'_{rrr}	6.10	4.80	4.78
14	$X'_{u\|v\|}$	68.	14.2	34.6	33	N'_{rrv}	5.23	5.20	5.24
15	Y'_{uv}	11	4.34	29.1	34	N'_{vvr}	1.73	1.77	2.49
16	Y'_{ur}	12	1.69	41.8	35	$N'_{v\|r\|}$	3.46	3.55	3.54
17	Y'_{uur}	12	2.83	6.15	36	$N'_{v\|v\|}$	0.31	0.31	0.31
18	Y'_{uuv}	10	1.95	4.53	37	$N'_{r\|v\|}$	0.98	0.50	0.50
19	Y'_{vvv}	13	17.2	34.6	38	$N'_{r\|r\|}$	10.8	147	162

CONCLUSIONS

This paper discussed the parameter uncertainty (also called parameter drift) of a nonlinear manoeuvring mathematical model of a marine surface ship in 3-DOF and truncated singular values decomposition and Tikhonov regularization were employed to diminish the uncertainty. First, a nonlinear manoeuvring mathematical model of a marine surface ship in 3-DOF was derived using Lagrange's method. In order to compare the coefficients of different ships, the hydrodynamic coefficients have been converted to the dimensionless ones using the prime system of SNAME (1950). A series of captive model tests were carried out by SINTEF Ocean (Ocean) on the scaled ship model according to the recommended procedures by ITTC, the data was used for the parameter estimation of the manoeuvring model and validation.

The classical parameters estimation method, Least Squares method, is briefly introduced, and the uncertainty of the hydrodynamic coefficients due to the noise in the measured data is analysed using singular value decomposition. The parameters with large uncertainty are very sensitive to the noise and easily drift the true values. A mathematical explanation for the parameter uncertainty or parameter drift was given using singular values decomposition. The estimation of the hydrodynamic manoeuvring coefficients is a typically ill-posed problem, so, truncated singular values decomposition and Tikhonov regularization was employed to reduce the uncertainty and diminish the parameter drift. The nondimensionalized hydrodynamic coefficients were obtained using a Least Squares method, truncated singular values decomposition and Tikhonov regularization based on PMM test data. The performance of the resulting nonlinear manoeuvring models was further tested against the portion of the data, which was not used in the identification process. The R^2 goodness of fit criterion was used to demonstrate the accuracy of the obtained models. Identification of the uncertain parameters using truncated singular values decomposition and Tikhonov regularization resulted in good estimating the parameters with smaller uncertainty.

ACKNOWLEDGEMENTS

This work was performed within the Strategic Research Plan of the Centre for Marine Technology and Ocean Engineering (CENTEC), which is financed by Portuguese Foundation for Science and Technology (Fundação para a Ciência e Tecnologia-FCT) under contract UID/Multi/00134/2013 - LISBOA-01-0145-FEDER-007629. This work was partly supported by the Research Council of Norway through the Centres of

Excellence funding scheme, Project number 223254 - AMOS. The first author is grateful to Prof. Asgeir Johan Sørensen, and Prof. Thor I. Fossen, who are the directors of NTNU-AMOS, for generous support and valuable discussion during his visit to AMOS NTNU. This work is a contribution to the project M&MSHIPS -"Maneuvering & Moored SHIPS in ports" (PTDC/EMSTRA/5628/2014) funded by the Portuguese Foundation for Science and Technology.

REFERENCES

Abkowitz, M.A., 1980. Measurement of hydrodynamic characteristics from ship maneuvering trials by system identification. SNAME Trans. 88, 283–318.

Åström, K.J., Källström, C.G., 1976. Identification of ship steering dynamics. Automatica 12, 9–22.

Bell, J.B., Tikhonov, A.N., Arsenin, V.Y., 1978. Solutions of Ill-Posed Problems. Math. Comput. 32, 1320–1322.

Berge, S.P., Fossen, T.I., 2000. On the Properties of the Nonlinear Ship Equations of Motion. Math. Comput. Model. Dyn. Syst. 6, 365–381.

Chan, T.F., Hansen, P.C., 1990. Computing Truncated Singular Value Decomposition Least Squares Solutions by Rank Revealing QR-Factorizations. SIAM J. Sci. Stat. Comput. 11, 519–530.

Chen, T., Ljung, L., 2013. Implementation of algorithms for tuning parameters in regularized least squares problems in system identification. Automatica 49, 2213–2220.

Cortes, C., Vapnik, V., 1995. Support-Vector Networks. Mach. Learn. 20, 273–297.

Fernandes, D. de A., Sørensen, A.J., Pettersen, K.Y., Donha, D.C., 2015. Output feedback motion control system for observation class ROVs based on a high-gain state observer: Theoretical and experimental results. Control Eng. Pract. 39, 90–102.

Fossen, T.I., 2011. Handbook of Marine Craft Hydrodynamics and Motion Control. John Wiley & Sons, Ltd, Chichester, UK.

Fossen, T.I., Sagatun, S.I., Sørensen, A.J., 1996. Identification of dynamically positioned ships. Model. Identif. Control 17, 153–165.

Kirchhoff, G. 1869. Ueber die Bewegung eines Rotationskörpers in einer Flüssigkeit. J. für die reine und Angew. Math. 71, 237–262.

Golding, B., Ross, A., Fossen, T.I., 2006. Identification of nonlinear viscous damping for marine vessels, in: 14 Th IFAC Symposium on System Identification. Newcastle , Australia , 2006, pp. 332–337.

Golub, G.H., Hansen, P.C., O'Leary, D.P., 1999. Tikhonov Regularization and Total Least Squares. SIAM J. Matrix Anal. Appl. 21, 185–194.

Golub, G.H., Reinsch, C., 1970. Singular value decomposition and least squares solutions. Numer. Math. 14, 403–420.

Hansen, P., 1998. Rank-deficient and discrete ill-posed problems: numerical aspects of linear inversion. Soc. Ind. Appl. Math. 175–208.

Hansen, P.C., Johnston, P.R., 2001. The L-Curve and its Use in the Numerical Treatment of Inverse Problems, in: Computational Inverse Problems in Electrocardiography. pp. 119–142.

Hansen, P.C., O'Leary, D.P., 1993. The Use of the L-Curve in the Regularization of Discrete Ill-Posed Problems. SIAM J. Sci. Comput. 14, 1487–1503.

Hassani, V., Fathi, D., Ross, A., Sprenger, F., Selvik, Ø., Berg, T.E.T.E., Fathi, D., Sprenger, F., Berg, T.E., 2015. Time domain simulation model for research vessel Gunnerus, in: Proceedings of the International Conference on Offshore Mechanics and Arctic Engineering - OMAE. ASME, p. V007T06A013.

Hassani, V., Sørensen, A.J., Pascoal, A.M., 2013. Adaptive wave filtering for dynamic positioning of marine vessels using maximum likelihood identification: Theory and experiments, in: IFAC Proceedings Volumes (IFAC-PapersOnline). pp. 203–208.

Hou, X.-R., Zou, Z.-J., Liu, C., 2018. Nonparametric identification of nonlinear ship roll motion by using the motion response in irregular waves. Appl. Ocean Res. 73, 88–99.

Hwang, W., 1980. Application of System Identification to Ship Maneuvering. Massachusetts Institute of Technology.

ITTC, 2002. Manoeuvrability Captive Model Test Procedure, in: The 23rd International Towing Tank Conference.

Liu, J., Hu, Y., Xu, C., Jiang, C., Han, X., 2016. Probability assessments of identified parameters for stochastic structures using point estimation method. Reliab. Eng. Syst. Saf. 156, 51–58.

Liu, J., Meng, X., Zhang, D., Jiang, C., Han, X., 2017. An efficient method to reduce ill-posedness for structural dynamic load identification. Mech. Syst. Signal Process. 95, 273–285.

Ljung, L., 1999. System identification : theory for the user. Prentice Hall PTR.

Luo, W., 2016. Parameter Identifiability of Ship Manoeuvring Modeling Using System Identification. Math. Probl. Eng. 2016, 1–10.

Luo, W., Guedes Soares, C., Zou, Z., 2016. Parameter Identification of Ship Maneuvering Model Based on Support Vector Machines and Particle Swarm Optimization. J. Offshore Mech. Arct. Eng. 138(3), 031101.

Luo, W., Li, X., 2017. Measures to diminish the parameter drift in the modeling of ship manoeuvring using system identification. Appl. Ocean Res. 67, 9–20.

Luo, W., Moreira, L., Guedes Soares, C., 2014. Manoeuvring simulation of catamaran by using implicit models based on support vector machines. Ocean Eng. 82, 150–159.

Luo, W.L., Zou, Z.J., 2009. Parametric Identification of Ship Maneuvering Models by Using Support Vector Machines. J. Sh. Res. 53, 19–30.

Lurie, A.I., 2002. Analytical Mechanics. Springer Berlin Heidelberg.

Ma, D., Tan, W., Zhang, Z., Hu, J., 2017. Parameter identification for continuous point emission source based on Tikhonov regularization method coupled with particle swarm optimization algorithm. J. Hazard. Mater. 325, 239–250.

Moreira, L. and Guedes Soares, C. 2003. Dynamic Model of Manoeuvrability using Recursive Neural Networks. Ocean Engineering. 30(7):1669-1697.

Moreira, L. and Guedes Soares, C. 2011. Guidance and Control of Autonomous Vehicles. Guedes Soares, C. Garbatov Y. Fonseca N. & Teixeira A. P., (Eds.). Marine Technology and Engineering. London, UK: Taylor & Francis Group ; pp. 503-520.

Nomoto, K., Taguchi, K., Honda, K., Hirano, S., 1956. On the Steering Qualities of Ships. J. Zosen Kiokai 1956, 75–82.

Ocean, SINTEF Ocean formerly known as Norwegian Marine Technology Research Institute-MARINTEK. [WWW Document]. URL https://www.sintef.no/en/ocean/ (accessed 4.26.18).

Perera, L. P.; Oliveira, P., and Guedes Soares, C. 2012. Maritime Traffic Monitoring based on Vessel Detection, Tracking, State Estimation, and Trajectory Prediction. Transactions on Intelligent Transportation Systems (IEEE). 13(3):1188-1200.

Perera, L.P., Oliveira, P., Guedes Soares, C., 2016. System identification of vessel steering with unstructured uncertainties by persistent excitation maneuvers. IEEE J. Ocean. Eng. 41, 515–528.

Perera, L.P., Oliveira, P., Guedes Soares, C., 2015. System Identification of Nonlinear Vessel Steering. J. Offshore Mech. Arct. Eng. 137, 031302.

Ridao, P., Carreras, M., Ribas, D., Sanz, P.J., Oliver, G., 2015. Intervention AUVs: The next challenge. Annu. Rev. Control 40, 227–241.

Ross, A., 2008. Nonlinear Manoeuvring Models for Ships: A Lagrangian Approach. NTNU.

Ross, A., Perez, T., Fossen, T.I., 2007. A novel manoeuvering model based on low-aspect-ratio lift theory and lagrangian mechanics. IFAC Proc. Vol. 40, 229–234.

Ross, A., Selvik, O., Hassani, V., Ringen, E., Fathi, D., 2015. Identification of Nonlinear Manoeuvring Models for Marine Vessels using Planar Motion Mechanism Tests, in: ASME 2015 34th International Conference on Ocean, Offshore and Arctic Engineering. p. V007T06A014-V007T06A014.

SimVal, Sea Trials and Model Tests for Validation of Shiphandling Simulation Models (SimVal) [WWW Document]. URL https://www.sintef.no/projectweb/simval/ (accessed 4.26.18).

SINTEF, Towing Tank - SINTEF [WWW Document]. URL https://www.sintef.no/en/all-laboratories/towing-tanks/ (accessed 4.26.18).

SNAME, 1950. Nomenclature for treating the motion of a submerged body through a fluid. Society of Naval Architects and Marine Engineers, New York.

Söderström, T., 2013. Comparing some classes of bias-compensating least squares methods. Automatica 49, 840–845.

Sørensen, A.J., 2011. A survey of dynamic positioning control systems. Annu. Rev. Control 35, 123–136.

Sutulo, S., Guedes Soares, C., 2006. Development of a Multifactor Regression Model of Ship Maneuvering Forces Based on Optimized Captive-Model Tests. J. Sh. Res. 50, 311–333.

Sutulo, S., Guedes Soares, C., 2011. Mathematical models for simulation of manoeuvring performance of ships, in: Guedes Soares, C., Garbatov, Y., Fonseca, N., Teixeira, A.P. (Eds.), Maritime Engineering and Technology. Taylor & Francis Group, London, pp. 661–698.

Sutulo, S., Guedes Soares, C., 2014. An algorithm for offline identification of ship manoeuvring mathematical models from free-running tests. Ocean Eng. 79, 10–25.

Sutulo, S., Guedes Soares, C., 2015a. Development of a core mathematical model for arbitrary manoeuvres of a shuttle tanker. Appl. Ocean Res. 51, 293–308.

Sutulo, S., Guedes Soares, C., 2015b. Offline System Identification of Ship Manoeuvring Mathematical Models with a Global Optimization Algorithm, in: MARSIM 2015. Newcastle, United Kingdom, pp. 8–11.

Suykens, J.A.K., Van Gestel, T., De Brabanter, J., De Moor, B., Vandewalle, J., 2002. Least Squares Support Vector Machines, World Scientific.

Suykens, J.A.K., Vandewalle, J., 1999. Least Squares Support Vector Machine Classifiers. Neural Process. Lett. 9, 293–300.

van de Ven, P.W.J., Johansen, T.A., Sørensen, A.J., Flanagan, C., Toal, D., 2007. Neural network augmented identification of underwater vehicle models. Control Eng. Pract. 15, 715–725.

Varela, J.M., Guedes Soares, C., 2015. Interactive 3D desktop ship simulator for testing and training offloading manoeuvres. Appl. Ocean Res. 51, 367–380.

Varela, J.M., Guedes Soares, C., 2015. Software architecture of an interface for three-dimensional collision handling in maritime Virtual Environments. Simulation 91, 735–749.

Xu, H.T., Guedes Soares, C., 2018a. An Optimized Energy-Efficient Path Following Algorithm for Underactuated Marine Surface Ship Model. Int. J. Marit. Eng. 160, A-411-A-421.

Xu, H.T., Hassani, V., Hinostroza, M.A., Guedes Soares, C., 2018b. Real-Time Parameter Estimation of Nonlinear Vessel Steering Model Using Support Vector Machine, in: ASME 2018 37th International Conference on Ocean, Offshore and Arctic Engineering. ASME, Madrid, Spain, p. V11BT12A009.

Xu, H.T., Hinostroza, M.A., Guedes Soares, C., 2018c. Estimation of Hydrodynamic Coefficients of a Nonlinear Manoeuvring Mathematical Model with Free-Running Ship Model Tests. Int. J. Marit. Eng. 160, A-213-A-226.

Xu, H.T., Guedes Soares, C., 2016. Vector field path following for surface marine vessel and parameter identification based on LS-SVM. Ocean Eng. 113, 151–161.

Yoshimura, Y., 2005. Mathematical model for manoeuvring ship motion (MMG Model), in: Workshop on Mathematical Models for Operations Involving Ship-Ship Interaction. Kansai Zōsen Kyōkai Kyōkai, pp. 1–6.